Neutron scattering function of vitreous and molten zinc chloride

1991 J. Phys.: Condens. Matter 3 9835

(http://iopscience.iop.org/0953-8984/3/49/001)

J. Phys.: Condens. Matter 3 (1991) 9835–9842. Printed in the UK

Neutron scattering function of vitreous and molten zinc chloride

David L Price, Marie-Louise Saboungi, Sherman Susman, Kenneth J Volin and Adrian C Wright†
Argonne National Laboratory, Materials Science Division, Argonne, IL 60439, USA

Received 15 July 1991, in final form 3 September 1991

Abstract. The dynamics of vitreous and molten zinc chloride have been studied with inelastic neutron scattering at the Intense Pulsed Neutron Source at Argonne National Laboratory. The results are analyzed in terms of the scattering function $S(Q, E)$ and the effective vibrational density of states $G(E)$. The vibrational spectra of both glass and liquid are dominated by broad features centred at 15 and 35 meV which are identified with the F_2 modes of $ZnCl_4^{2-}$ tetrahedra. The other two normal modes are not observed because of inadequate resolution and because of broadening and overlap resulting from coupling between tetrahedra. The energy widths of the scattering are lower than those predicted for independent particles over the entire Q range of the measurement, indicating strong binding of the ions to the network structure in both the glass and liquid.

1. Introduction

Zinc chloride, $ZnCl_2$, has a tetrahedrally coordinated network structure in both vitreous and liquid states. Its structure has been thoroughly established by neutron diffraction measurements in the glass by Desa *et al* [1] and in the liquid by Biggin and Enderby and by Howe *et al* [2]. It has also been investigated by molecular dynamics simulations [3], on the basis of solely ionic forces. Its bond angle of approximately 110° [1] places it intermediate between oxide glasses like SiO_2 (~140°) and chalcogenide glasses like $GeSe_2$ (~100°). From the point of view of transport properties, $ZnCl_2$ behaves as a relatively fragile liquid [4] compared with other tetrahedrally coordinated glass formers, having a rapid drop in viscosity as the temperature is raised above the glass transition, T_g (390 K).

Despite the considerable interest in the structural and transport properties of $ZnCl_2$, there has been relatively little inelastic neutron scattering work devoted to it. An early cold neutron study of liquid $ZnCl_2$ and other molten salts was carried out by Wilmshurst and Bracker [5], and Galeener *et al* made measurements on vitreous $ZnCl_2$ with a beryllium-filter spectrometer [6]. However, both these studies covered a restricted range of wave vector Q and only constant-angle data were presented. A high-resolution study made by Müller *et al* [7] to investigate the dynamics of the system at long times in the vicinity of the glass transition was confined to the quasielastic energy region. The aims

† Permanent address: J J Thomson Physical Laboratory, University of Reading, UK.

0953-8984/91/499835 + 08 $03.50

of the present study were to investigate the dynamics of the glass and liquid by measuring the scattering function $S(Q, E)$ over a wide range of energy E and wave vector Q and to compare the results with those of similar studies of vitreous SiO_2 [8], $GeSe_2$ [9] and $SiSe_2$ [10]. In addition, the low T_g of $ZnCl_2$ makes the liquid state more amenable to inelastic neutron scattering measurements than in the case of other tetrahedrally coordinated materials.

2. Experimental procedure

Samples of high-purity anhydrous $ZnCl_2$ were obtained from APL Engineered Materials Inc., Urbana, IL. An effective test of water content in $ZnCl_2$ is the structure of the crystallized material, since even minute water contamination will produce the hydrate structure instead of that of pure $ZnCl_2$ [1]. A sample of material from the supplied batch was therefore crystallized and measured by neutron powder diffraction on the Special Environment Powder Diffractometer at IPNS. Rietveld analysis revealed the δ–$ZnCl_2$ (orthorhombic) form of the pure material [11]. For the inelastic measurements, the sample material was contained in a row of 16 vitreous silica tubes, i.d. 3 mm, o.d. 4 mm, 150 mm long, placed at 45° in transmission to the incident beam.

The tubes were mounted in an aluminium frame in the sides of which two cartridge heaters were mounted, out of the beam area, to provide the required temperature for the liquid. All temperature differences across the sample were less than 15°. The beam dimensions were 50 mm wide by 100 mm high, and the tubes contained sufficient material to cover the height of the beam. The material supplied was a mixture of crystalline and amorphous phases; it was converted to the pure vitreous form by melting to 370 °C and quenching in water to room temperature. Optical inspection confirmed the vitreous nature of the sample, and no Bragg peaks were observed in the neutron measurements.

Inelastic neutron scattering measurements were carried out on the low-resolution medium-energy chopper spectrometer (LRMECS) at IPNS with an incident energy $E_0 = 80.3$ meV. Time-of-flight data were collected in 41 groups of detectors placed at mean scattering angles φ ranging from 2.7° to 116.4°. Runs were made with the $ZnCl_2$ sample in the vitreous state at 298 K (60 h) and in the liquid state at 620 K (51 h). This temperature, 230 K above the glass transition and 30 K above the melting point, T_m = 590 K, was chosen to avoid the possibility of crystallization. Runs were also made with an equivalent set of empty silica tubes at the same temperatures (40 and 45 h), with a vanadium standard (17 h), with no material in the beam (13 h), and with a cadmium absorber covering the sample (6 h). Data were converted to the form of the scattering function $S(Q, E)$ and effective vibrational density of states $G(E)$ using standard procedures described in detail by Price and Carpenter [8]. Energies will be quoted in meV: 1 meV is equivalent to a frequency $\omega = 1.52\ 10^{12}\ s^{-1}$ or a wavenumber $\bar{\nu} = 8.07\ cm^{-1}$. The energy resolution (FWHM) was 5.3 meV for elastic scattering ($E = 0$), decreasing to approximately 3.2 meV for energy transfers of 50 meV. The Q resolution was estimated to be 0.14 $Å^{-1}$ at $Q = 5\ Å^{-1}$.

3. Results

The neutron-weighted average scatering function for a multi-component system is a weighted sum of the partial coherent and incoherent scattering functions [12]:

Table 1. Atomic and nuclear parameters for $ZnCl_2$.

	Zn	Cl
Charge ($\|e\|$)	+2	−1
Ionic radius (Å) [20]	0.74	1.81
Mass (amu)	65.37	35.45
$4\pi\bar{b}^2(b)$ [21]	4.05	11.53
$4\pi(\overline{b^2}-\bar{b}^2)(b)$ [21]	0.08	5.2
$\sigma_{abs}(b)$ [21]	1.11	33.5

$$\langle S(Q,E)\rangle=\frac{1}{\langle\overline{b^2}\rangle}\left\{\sum_{dd'}c_d^{1/2}c_{d'}^{1/2}\bar{b}_d^*\bar{b}_{d'}S_c^{dd'}(Q,E)+\sum_d c_d(|\overline{b_d^2}|-|\bar{b}_d|^2)S_i^d(Q,E)\right\} \tag{1}$$

where c_d, $\bar{b}_d$, and $\overline{b_d^2}$ are the concentration, mean scattering length, and mean square scattering length (averaged over spins and isotopes) for element d and $\langle\overline{b^2}\rangle$ is the average of $\overline{b_d^2}$ over all elements. The appropriate nuclear parameters for $ZnCl_2$ are given in table 1.

A primary check on the inelastic scattering data is provided by integration over E at constant Q to give the neutron-weighted average structure factor $S(Q)$:

$$\langle S(Q)\rangle=\left\langle\frac{1}{\overline{b^2}}\right\rangle\left\{\sum_{dd'}c_d^{1/2}c_{d'}^{1/2}\bar{b}_d^*\bar{b}_{d'}S^{dd'}(Q)+\sum_d c_d(|\overline{b_d^2}|-|\bar{b}_d|^2)\right\}. \tag{2}$$

This satisfies the condition $\langle S(Q)\rangle\to 1$ as $Q\to\infty$. The average structure factors for glass and liquid are shown in figure 1. These differ from those measured in a diffraction measurement in that (i) incoherent and Laue diffuse scattering, both giving rise to a constant additive term, are included; (ii) the integration range of E is limited to $E=E_0$ at the upper end; (iii) the integration is carried out at constant Q so that the inelasticity corrections which have to be applied in a diffraction experiment are not needed. Nevertheless the $S(Q)$ results shown in figure 1 reproduce the published diffraction results for glass [1] and liquid [2] rather well, including the first peak at $Q=1$ Å^{-1}, which is equivalent to the first sharp diffraction peak (FSDP) for vitreous silica at 1.5 Å^{-1} but is not so pronounced because of the dominant scattering length of the Cl atoms (cf figure 7 of [13]).

The same features show up in the energy-analyzed elastic scattering, the main difference from the behavior of $S(Q)$ in figure 1 being the fall-off in the intensity at large Q, due to the larger proportion of scattering occurring at larger E as Q increases.

The energy dependence of the inelastic scattering is most easily visualized from the effective neutron- and amplitude-weighted vibrational density of states $G(E)$ [8]. For the glass, multiphonon scattering was subtracted with an iterative procedure [8] to give the function $G_1(E)$ shown in figure 2, which represents the best estimate of the effective one–phonon density of states for the glass. The low-E region, where the elastic scattering falls within the resolution function, has been excluded. $G_1(E)$ is seen to be dominated by two peaks centred approximately at 15 and 35 meV (~120 and 280 cm^{-1}) respectively. The same two features were observed by Galeener *et al* [6] although the first peak occurs at a slightly lower energy (~11 meV) in their data.

In the Raman scattering data of Galeener *et al* [6], the spectrum with HV polarization, which usually resembles the true density of states [14], shows principal peaks at 110 and

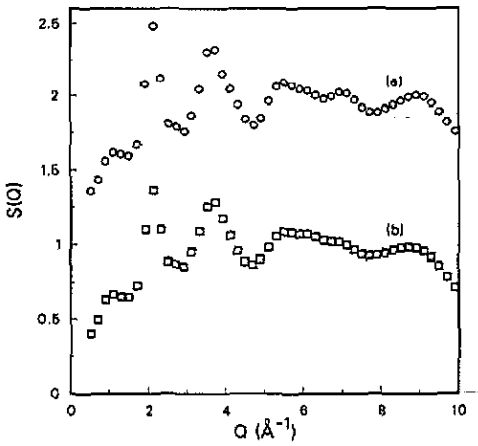

Figure 1. Average structure factors $\langle S(Q)\rangle$ for $ZnCl_2$: (*a*) glass at 298 K and (*b*) liquid at 620 K, obtained by integrating $\langle S(Q, E)\rangle$ over energy. Curve (*a*) is displaced vertically by 1.0 unit.

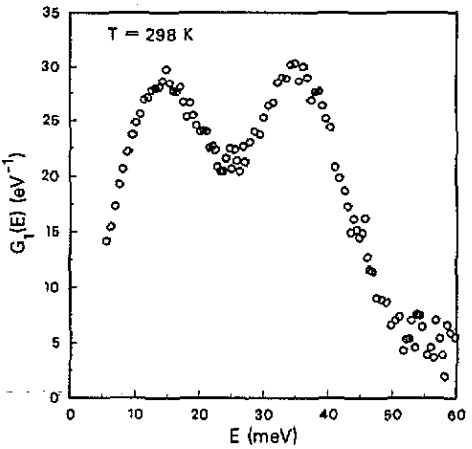

Figure 2. One-phonon effective vibrational density of states $G_1(E)$ for vitreous $ZnCl_2$.

280 cm^{-1}, in good agreement with the peaks in the neutron measurement. Smaller peaks are observed around 80, 230 and 320 cm^{-1}; the peak at 230 cm^{-1} dominates the HH spectrum. By analogy with $GeSe_2$ [9], which has a rather similar spectrum, the latter can be identified with the A_1 tetrahedral breathing mode. Peaks at similar energies are observed in the later measurements of Cacciola *et al* [15], who identify the peaks around 70, 100–120, 230 and 270–320 cm^{-1} in the glass with tetrahedral modes of $E(\nu_2)$, $F_2(\nu_4)$, $A_1(\nu_1)$, and $F_2(\nu_3)$ symmetry, respectively. The splitting of the two F_2 modes is ascribed to TO–LO splitting. In the neutron effective density of states, only the two F_2 modes appear to be present. The same features, slightly shifted, are observed in the Raman spectra of the liquid at 592 K.

The far-infrared spectra measured by Angell *et al* [16] for $ZnCl_2$ glass and liquid show features generally similar to the Raman spectra. In the glass at room temperature, the principal peaks are at 105 and 265 cm^{-1} with shoulders at 75 and 120 cm^{-1}; in the liquid at 593 K, the principal peaks are at 90 and 260 cm^{-1} with a shoulder around 120 cm^{-1}. The main difference from the Raman spectra is that the several Raman peaks observed in the 230–320 cm^{-1} region in both glass and liquid are replaced by a broad spectrum centered around 260 cm^{-1}.

Sen and Thorpe [17] have shown that, under a certain set of simplifying conditions, the dynamics of AX_2 glasses can be described in terms of the AX_4 tetrahedra. A necessary condition for this to be applicable is that the AXA bond angle θ lies below the critical value $\theta_c = \cos^{-1}(-2M_X/3M_A)$, which has the value 111.2° for $ZnCl_2$, very close to the observed value of θ. Nevertheless, if we adopt this approach, the frequencies and structure factors of the normal modes can be calculated in terms of isolated AX_4 tetrahedra following the procedure followed for $GeSe_2$ in [9]. With values for the two valence force constants of $f_1''' = 110$ and $f_2''' = 30$ N m^{-1} (bond-bending and bond-stretching, respectively), we obtain frequencies for the four tetrahedral modes of 104 (E), 112 (F_2), 230 (A_1) and 310 (F_2) cm^{-1}, respectively, in reasonable agreement with the optical frequencies and with the two neutron peaks, if these are ascribed to

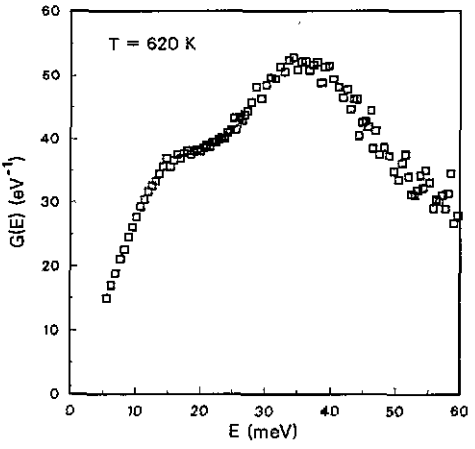

Figure 3. Effective vibrational density of states $G(E)$ for liquid $ZnCl_2$.

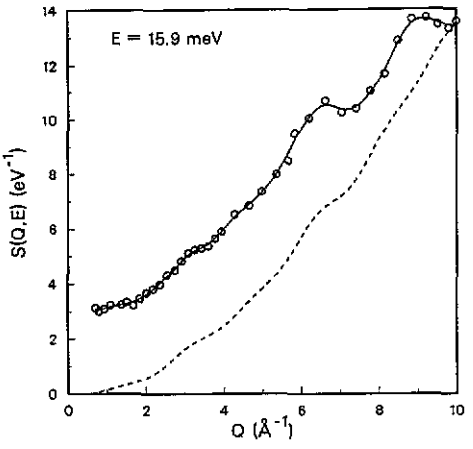

Figure 4. Scattering function $\langle S(Q, E)\rangle$ for vitreous $ZnCl_2$ measured at $E = 15.9$ meV (symbols), compared with model calculations for the ν_4 mode (broken curve). The full curve through the symbols represents a smooth cubic spline fit to the data.

the two modes of F_2 symmetry. We discuss below the structure factors of these two modes.

Figure 3 shows the total effective density of states $G(E)$ for the liquid, which is related to the Fourier transform of the weighted average velocity autocorrelation function [12]. In spite of the difference in the state of the sample, the functions shown in figures 3 and 4 have some similarity. (The fact that $G_1(E)$ is shown for the vitreous state and $G(E)$ for the liquid is not very significant, since the multiphonon scattering appears as a smoothly varying background under the one-phonon scattering from the glass.) In particular, the features at 15 and 35 meV observed in the glass survive the melting process, confirming the conclusion of Biggin and Enderby that the $ZnCl_4^{2-}$ tetrahedra continue to play a significant role in the structure of the liquid.

The wave-vector dependence of the inelastic scattering is best viewed by considering the Q dependence of $S(Q, E)$ for a particular energy E. For the present purpose, we examine the scattering associated with the main peaks in $G(E)$. Figures 4 and 5 show the Q dependence of $S(Q, E)$ for the glass at energies $E = 15.9$ and 35.6 meV, respectively. The Q dependence shows the expected Q^2 dependence at small Q, followed by the drop-off at high Q arising from the Debye–Waller factor, with a small amount of short-period oscillation, which can be ascribed to correlated displacements of nearby atoms in the normal modes of vibration [8, 9]. In figures 5 and 6 we show the structure factors for the $F_2(\nu_4)$ and $F_2(\nu_3)$ modes computed with the tetrahedral model discussed above. There are some similarities between the observed and calculated structure factors but the agreement is not as striking as in the case of $GeSe_2$ [9], perhaps because the condition for the validity of the isolated tetrahedral model ($\theta \ll \theta_c$) is not as well fulfilled. We note that $SiSe_2$ [10] also does not agree as well with the isolated tetrahedral model, perhaps because the tetrahedra are predominantly edge-sharing and therefore more strongly coupled. For SiO_2, on the other hand, $\theta > \theta_c$ and the dynamics are more suitably discussed in terms of OSi_2 units [8].

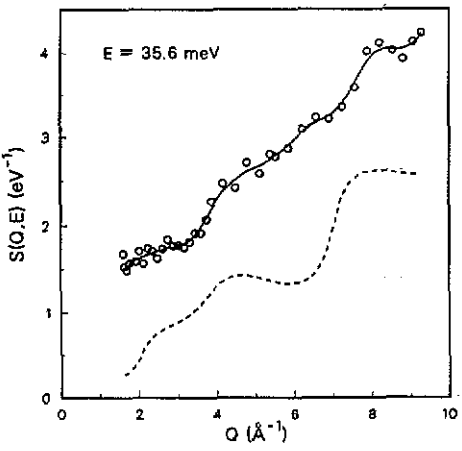

Figure 5. Scattering functions $\langle S(Q, E)\rangle$ for vitreous $ZnCl_2$ measured at $E = 35.6$ meV (symbols), compared with model calculations for the ν_3 mode (broken curve). The notation is the same as for figure 5.

The value of the bond angle in $ZnCl_2$ may account for the fact that only two peaks are visible in the density of states $G_1(E)$ as measured by neutron scattering, compared with the four or more observed for $GeSe_2$ [9]. Sen and Thorpe [17] showed that, as θ approaches θ_c, the $\nu_1(A_1)$ and $\nu_3(F_2)$ tetrahedral modes broaden and in factor overlap at $\theta = \theta_c$, the condition that applies for $ZnCl_2$. In particular, the delta-function component of the $\nu_1(A_1)$ mode overlaps with the continuous component of the $\nu_3(F_2)$. This appears to make the $\nu_1(A_1)$ mode indistinguishable in the neutron density of states. The lower two tetrahedral modes, $E(\nu_2)$ and $F_2(\nu_4)$ are, according to the optical data [14, 15], separated by about 30 cm^{-1} which is less than the resolution of the present measurement. The shoulder which can be barely identified in the neutron density of states at 11 meV (90 cm^{-1}) may be an indication of the $E(\nu_2)$. The marked difference in scattering lengths may be another factor in determining peak intensities.

Finally, we discuss the energy width of the scattering at a particular Q in terms of the full width at half maximum $\Delta(Q)$. The second energy moment of the average scattering function for a classical system is given by

$$\langle E^2\rangle = \hbar^2 Q^2 k_B T \left(\sum_d c_d |\overline{b_d^2}| M_d^{-1}\right) \Big/ \langle \overline{b^2}\rangle \tag{3}$$

and, if $S(Q, E)$ has a purely Gaussian shape, then $\Delta(Q)$ is given by

$$\Delta(Q) = 2.355[\langle E^2\rangle / \langle S(Q)\rangle]^{1/2}. \tag{4}$$

The reduction in $\Delta(Q)$ at peaks in $S(Q)$ is the familiar de Gennes narrowing [18]. The experimental values of $\Delta(Q)$ are shown in figures 6 and 7 for glass and liquid, respectively, compared with the Gaussian values given by equation (4). The experimental values are obtained from the measured spectra by deconvolving the experimental resolution. We note that the general behaviour is similar but the measured values of the FWHM are lower than those of the equivalent Gaussian. This implies a scattering function which, relative to the Gaussian curve of the same area and variance, has a peaked low-frequency portion and a slowly decaying high-frequency portion. This shape is a quite typical behaviour for a classical liquid and was, in fact, postulated by de Gennes [18] on the basis of moment relations. In terms of the decay of the density fluctuations with time, it implies a rapid initial decrease of the amplitude of the fluctuation followed by a period in which it decays

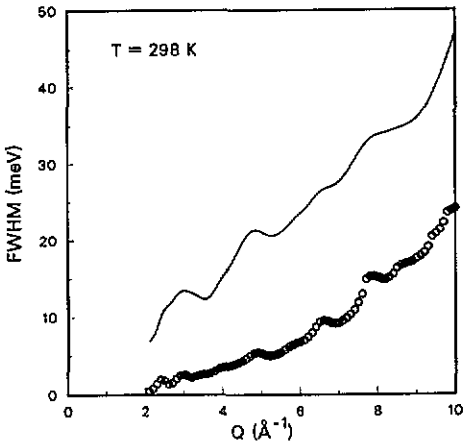

Figure 6. Energy full width at half-maximum for vitreous $ZnCl_2$ (symbols), compared with a Gaussian calculation (full curve).

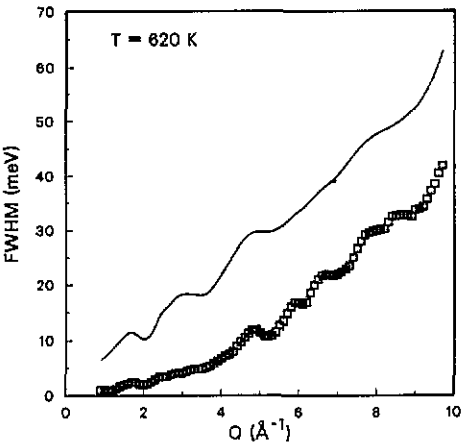

Figure 7. Energy full width at half-maximum for liquid $ZnCl_2$ (symbols), compared with a Gaussian calculation (full curve).

more slowly, a behaviour which is relatively more pronounced near the peak of the structure factor. For larger values of Q the ratios approach unity as the scattering functions acquire the Gaussian shape corresponding to the independent-particle regime. However, this limit is not reached for either vitreous or liquid $ZnCl_2$ by 10 Å^{-1}, the highest Q in this experiment. This behaviour is in marked contrast to other molten salts, for example RbBr [19], where Gaussian behaviour is reached by 5 Å^{-1}, presumably because $ZnCl_2$ is a network system with a viscosity orders of magnitude higher than molten RbBr, so that single-particle behaviour is only reached at much shorter times. In the case of the glass, it is interesting that the scattering function consists of a single broad peak, with no resolvable elastic scattering, for Q values as low as 2 Å^{-1}, in contrast to other glasses such as SiO_2 [8] and $GeSe_2$ [9] where elastic scattering could be resolved over the entire Q range.

4. Concusions

The vibrational spectra of both vitreous and liquid $ZnCl_2$ are dominated by broad features centred at 15 and 35 meV. These features are ascribed to the two F_2 modes of the $ZnCl_4^{2-}$ tetrahedra. The other two normal modes are not observed, the lower one possibly due to inadequate resolution, the upper perhaps because of broadening and overlap resulting from coupling between tetrahedra, which is expected to be strong because the bond angle is nearly equal to the critical angle for inter-tetrahedral coupling.

The energy widths of the inelastic scattering for both glass and liquid follow the general pattern predicted by de Gennes but with values for the FWHM substantially below the values predicted for independent particles over the entire Q range of the measurement. This is ascribed to the strong binding of the ions to the network structure in both the vitreous and liquid states.

Acknowledgments

We wish to thank R Kleb for design and construction of the cartridge heater furnace, T Brumleve of APL Engineering Materials Inc. for providing high quality, anhydrous material, and the operations staff of the Intense Pulsed Neutron Source for experimental assistance. We acknowledge helpful discussions with C A Angell, J M Carpenter, J E Enderby, C-K Loong, R McGreevy and R O Pohl. This work was performed under the auspices of the US Department of Energy, Division of Materials Science, Office of Basic Energy Sciences, under Contract W-31-109-ENG-38.

References

[1] Desa J A E, Wright A C, Wong J and Sinclair R N 1982 *J. Non-Cryst. Solids* **51** 57
[2] Biggin S and Enderby J E 1981 *J. Phys. C: Solid State Phys.* **14** 3129
Allen D A, Howe R A, Wood N D and Howells W S unpublished
[3] Woodcock L V, Angell C A and Cheeseman P 1976 *J. Chem. Phys.* **65** 1565
[4] Angell C A 1988 *J. Non-Cryst. Solids* **102** 205
[5] Wilmshurst J K and Bracker J M 1969 *Molten Salts, Characterization and Analysis* ed G Mamantov (New York: Dekker) p 291
[6] Galeener F L, Mikkelsen J C, Wright A C, Sinclair R N, Desa J A E and Wong J 1980 *J. Non-Cryst. Solids* **42** 23
[7] Müller P, Jung S and Heidemann A 1988 *Z. Phys. Chem.* **156** 403
[8] Price D L and Carpenter J M 1987 *J. Non-Cryst. Solids* **92** 153
Arai M, Hannon A C, Taylor A D, Wright A C, Sinclair R N and Price D L unpublished
[9] Walter U, Price D L, Susman S and Volin K J 1988 *Phys. Rev.* B **37** 4232
[10] Arai M, Price D L, Susman S, Volin K J and Walter U 1988 *Phys. Rev.* B **37** 4240
[11] Franklin S V, Price D L and Richardson J W 1989 *Student Report* Argonne National Laboratory
[12] Price D L and Sköld K 1986 *Neutron Scattering (Methods of Experimental Physics 23 A)* ed K Sköld and D L Price (Orlando, FL: Academic) p 1
[13] Wright A C 1987 *Wiss. Z. Friedrich-Schiller-Univ. Jena, Naturwiss. Reihe* **36** 943
[14] Galeener F L, Leadbetter A J and Stringfellow M W 1983 *Phys. Rev.* B **27** 1052
[15] Cacciola M L, Magazu S, Migliardo P, Aliotta F and Vasi C 1986 *Solid State Commun.* **57** 513
[16] Angell C A, Wegdam G H and Van der Elsken J 1974 *Spectrochimica Acta* **30A** 665
Angell C A and Wong J 1970 *J. Chem. Phys.* **53** 2053
[17] Sen P N and Thorpe M F 1977 *Phys. Rev.* B **15** 4030
[18] de Gennes P G 1959 *Physica* **25** 825
[19] Price D L and Copley J R D 1975 *Phys. Rev.* B **11** 2124
[20] Pauling L 1960 *Nature of the Chemical Bond* (Ithaca: Cornell University Press)
[21] Sears V F 1986 *Neutron Scattering (Methods of Experimental Physics 23 A)* ed K Sköld and D L Price (Orlando, FL: Academic) p 521